Synthesis, Structure, and Biological Activity of des-Side Chain Analogues of 1α,25-Dihydroxyvitamin D_3 with Substituents at C-18

Lieve Verlinden,[†] *Annemieke Verstuyf,*[†] *Guy Eelen,*[†] *Roger Bouillon,*[†] *Paloma Ordóñez-Morán,*[‡] *María Jesús Larriba,*[‡] *Alberto Muñoz,*[‡] *Natacha Rochel,*[§] *Yoshiteru Sato,*[§] *Dino Moras,*[§] *Miguel Maestro,*[∥] *Samuel Seoane,*[ƒ] *Fernando Dominguez,*[ƒ] *Silvina Eduardo-Canosa,*[#] *Daniel Nicoletti,*[#] *Edelmiro Moman,*[#] *Antonio Mouriño.*[#,*]

[†] Laboratorium voor Experimentele Geneeskunde en Endocrinologie, Katholieke Universiteit Leuven, B-3000 Leuven, Belgium, [‡] Instituto de Investigaciones Biomédicas, "Alberto Sols", Consejo Superior de Investigaciones Científicas-Universidad Autónoma de Madrid, E-28029 Madrid, Spain, [§] IGBMC, Département de Biologie et de Génomiques Structurales, F-67400 Illkirch, France, [∥] Departamento de Química Fundamental, Universidad de A Coruña, E-15071 A Coruña, Spain, [ƒ] Departamento de Fisiología, Facultad de Medicina, Universidad de Santiago, E-15782 Santiago de Compostela, Spain, [#] Departamento de Química Orgánica y Unidad Asociada al CSIC, Universidad de Santiago, E-15782 Santiago de Compostela, Spain

RECEIVED DATE

- To whom correspondence should be addressed. Phone, +34 600942435; fax, +34 981595012, E-mail, antonio.mourino@usc.es.
- Antonio Mouriño dedicates this paper to Argentinean Professors Rita H. Rossi, Julio C. Podestá, Manuel González Sierra and Oscar S. Giordano, for their dedication and contribution to organic chemistry.

ABBREVIATIONS LIST. DBP: vitamin D binding protein, VDR: vitamin D receptor, VDRE: vitamin D response element

ABSTRACT An improved synthetic route to des-side chain analogues of 1α,25-dihydroxyvitamin D_3 with substituents at C-18 and their biological activity is reported. These analogues displayed significant antiproliferative and prodifferentiating effects with a greatly reduced calcemic profile. The crystal structure of the human vitamin D receptor (hVDR) complexed to one of these analogues, 20(17→18)-abeo-1α,25-dihydroxy-22-homo-21-norvitamin D_3 (**2a**), revealed that the side chain introduced at position C-18 adopts the same orientation in the ligand binding pocket as the side chain of 1α,25-dihydroxyvitamin D_3.

Introduction

The growth-inhibitory, prodifferentiating, and immunomodulatory activity of 1α,25-dihydroxyvitamin D_3 (**1a**, Fig. 1), the hormonally active form of vitamin D_3 (**1b**), opens perspectives for the use of this compound in cancer, psoriasis, and immune-related disorders such as multiple sclerosis and inflammatory bowel disease. However, the therapeutic applicability of 1α,25-dihydroxyvitamin D_3 is limited due to hypercalcemia.[1] Therefore, it remains a major challenge to design and synthesize analogues of 1α,25-dihydroxyvitamin D_3 that have the best possible balance between the advantageous antiproliferative and prodifferentiating effects and the adverse calcemic activity.

One of our research strategies is focused on the synthesis of 1α,25-

dihydroxyvitamin D_3-analogues with side chains attached to the angular C-18 methyl group. Most of the reported C-18 substituted analogues are linked to C-18 through an oxygen atom and carry residual groups at C-17.[2] We recently reported the synthesis of novel 1α,25-dihydroxyvitamin D_3-analogues in which side chains homologous to that of the natural hormone are linked to C-18 through a C-C bond and that have no substituents on C-17.[3] However, the structural analysis and biological activity of these compounds was not yet reported. In this paper we present an improved synthetic route to two of these analogues, 20(17→18)-abeo-1α,25-dihydroxy-22-homo-21-norvitamin D_3 (**2a**, Fig. 1) and 20(17→18)-abeo-1α,25-dihydroxy-22,23-dihomo-21-norvitamin D_3 (**2b**). A structural study of the 7-membered C-18 side chain analogue **2a** complexed to hVDR was performed in order to investigate the binding mode of this newly introduced side chain at C-18. Furthermore, the biological activity profile of these analogues was determined in several cancer cell lines.

Results and discussion

Chemistry. The target compounds **2a** and **2b** were synthesized by modified procedures of our previous strategy[3] as outlined in Scheme 1. The replacement of the *tert*-butyldimethylsilyl protecting group by the triethylsilyl group was thought to have benefits at the final deprotection-purification stage. To set the vitamin D triene system corresponding to **2a**, we coupled hydroxyketone **4** with the lithium anion of phosphine oxide **3** in THF at -78 ºC to obtain protected vitamin D_3 analogue **2a-TES** in 85% yield. Desilylation of **2a-TES** took place cleanly using pyridinium fluoride to give the desired vitamin D_3 analogue **2a** in high yield. This result validates the use of phosphine oxide **3** in the syntheses of

future vitamin D_3 analogues following Lythgoe's Wittig-Horner approach.[4] The synthesis of **2b** commenced with known carboxylic acid **5**,[3] which was converted to alcohol **6** in 24% yield by a seven-step sequence involving reduction of the carboxylic group, tosylation, displacement of the resulting tosylate with sodium cyanide, reduction of the resulting nitrile to the homologated aldehyde, methylation, oxidation and methylation of the resulting ketone. Desilylation of **6** followed by hydrogenation of the double bond and oxidation of the secondary hydroxyl group provided ketone **7** in 82% yield. Coupling of ketone **7** with the lithium anion of phosphine oxide **3** afforded, after desilylation, the desired eight-membered vitamin D side-chain analogue **2b** in 78% yield over the three steps (12 steps from **5**, 15.7% overall yield).

Structural analysis. A structural study of the hVDR-**2a** complex was performed to gain more insight in the interaction of the **2a** analogue with the VDR. In this complex, the protein adopted the canonical conformation of all previously reported structures of VDR bound to agonist and superagonist ligands with helix H12 folded in the agonistic position.[5] The 7-membered side chain introduced at position C-18 adopted the same orientation in the pocket. An adaptation of its conformation was observed to maintain the hydrogen bonds forming the anchoring points. Compared with the structure of hVDR-1α,25$(OH)_2D_3$ complex, the atomic coordinates of hVDR bound to compound **2a** showed root-mean-square deviation of 0.25 Å of all Cα atoms. The sizes of the ligands were 391 and 396 $Å^3$ for analogue **2a** and 1α,25$(OH)_2D_3$, respectively. The volume of the ligand binding cavity was 638 and 673 $Å^3$ and the ligand occupied 59% and 61% of the pocket for **2a** and 1α,25$(OH)_2D_3$,

respectively. The A and secoB rings of the C-18 side chain analogue **2a** presented conformations similar to those of the natural ligand (Fig. 2A-B). As a consequence of the modified side chain, the C and D rings were shifted by around 0.4 Å. The distance between the 1-hydroxy and the 25-hydroxy groups varied from 13.1 Å for 1α,25(OH)$_2$D$_3$ to 12.8 Å for analogue **2a** complex. All the residues of VDR forming the binding pocket adopted the same conformation as those of the VDR/1α,25(OH)$_2$D$_3$ except for the side chain of Ile271 (H5). The interactions between the ligand and the receptor involved hydrophobic contacts and electrostatic interactions. The hydroxyl groups made the same hydrogen bonds as VDR/1α,25(OH)$_2$D$_3$ complex, 1-OH with Ser237 (H3) and Arg274 (H5), 3-OH with Tyr143 (H1) and Ser278 (β0), and the 25-OH with His305 (loop H6-H7) and His397 (H11). Because of the modification of the ligand, the side chain of compound **2a** took another pathway in the pocket and made additional contacts with the CB atom of Leu230 (H3) at 3.9 Å of C-20 and 3.6 Å of C-22 atom, respectively. Its side chain, however, lost a contact with the CD2 atom of Leu309 (H7) at 3.8 Å of C-21 for 1α,25(OH)$_2$D$_3$ (Fig. 2C). The elongated side chain of **2a** induced contacts between the C-26 and Leu404 (H11), the C-26 and Leu414 (loop H11-H12), C-27 and Phe422 (H12) at the end of the ligand. A Cα atom of His305 was shifted by 0.4 Å to maintain the hydrogen bonds with the hydroxyl group.

To confirm the crystallographic data, several VDR mutants were used to investigate the capacity of compound **2a** to transactivate a vitamin D response element (VDRE)-containing reporter construct. 1α,25(OH)$_2$D$_3$ as well as the 7-membered C-18 side chain analogue **2a** were unable to transactivate the

reporter construct when cells were transfected with VDRs carrying either the Leu233Ala, Ile271Ala, Arg274Ala, Trp286Ala, His397Ala, or Tyr401Ala mutation (Fig. 3). The transactivation potency of 1α,25$(OH)_2D_3$ was moderately reduced when cells were transfected with the VDR mutants Val234Ala, Ile268Ala, Val300Ala, and His305Ala (50% of the activity of wild type VDR), whereas transfection with the mutants Ser275Ala and Ser278Ala had little effect on the transactivation capacity of 1α,25$(OH)_2D_3$. Introduction of a 7-membered side chain at C-18 rendered analogue **2a** less potent than 1α,25$(OH)_2D_3$ in transactivating a VDRE-containing reporter construct in cells transfected with the VDR mutants Ile268Ala, Ser275Ala, Val300Ala, and His305Ala. These findings were in agreement with the crystal structure and suggested that interactions with these amino acids became more critical when a side chain was introduced at C-18 instead of at position C-17. The transactivating capacity of the VDR mutant Val234Ala became more potent in cells that were incubated with compound **2a**, which confirmed crystallographic data that showed a weaker interaction between this amino acid and the side chain of this **2a** analogue.

Heterodimerization with RXR. To assess whether VDR bound to DSA was able to heterodimerize with RXR, we monitored its interaction with by ESI-MS under non-denaturating conditions. Addition of fivefold molar excess of **2a** in the heterodimer VDR/RXR LBDs resulted in the appearance of a novel series of mass/charge (m/z) ions corresponding to a fully bound VDR-**2a**/RXR.[6] The different conformation of the VDR-bound **2a** analogue does not affect the VDR/RXR heterodimer stability. We then monitored by ESI-MS the

recruitment of the SRC-1 NR2 coactivator peptide to VDR-**2a**/RXR complex (data not shown) that was similar to VDR- 1α,25(OH)$_2$D$_3$/RXR.

Biological evaluation. Despite the fact that the analogue **2a** fitted well in the VDR binding pocket and that the hydrogen bonds, which form the anchoring points, were maintained, the affinity of compound **2a** for pig VDR was greatly reduced (2.5% of the affinity of 1α,25(OH)$_2$D$_3$) (Table 1). Also the binding to the transport protein vitamin D binding protein (hDBP) was significantly reduced (10% of the affinity of 1α,25(OH)$_2$D$_3$). Homologation of the side chain in compound **2b** further decreased the binding affinity to DBP and VDR (1.3% and 4% of the affinity of 1α,25(OH)$_2$D$_3$, respectively). The low affinity for the DBP can be explained by attachment of the **2a** and **2b** side-chain fragments to the C18 that orientates the side-chain hydroxyl groups towards the β-face of the CD rings. The lower affinity of **2a** and **2b** for DBP may also explain their reduced calcemic activity. Nothwithstanding this low affinity for VDR, but in accordance with the transactivation results, the 7-membered C-18 side chain analogue **2a** was as potent as 1α,25(OH)$_2$D$_3$ in reducing the proliferation of human breast adenocarcinoma MCF-7 cells (Table 1). Addition of an extra C-atom in the side chain in compound **2b** decreased the growth-inhibitory potential of this analogue because 3-fold higher concentrations of this compound were required to obtain a 50% decrease in proliferation. The ability to induce cell differentiation was investigated in human colon cancer SW480-ADH cells, which upon incubation with 1α,25(OH)$_2$D$_3$ undergoes epithelial differentiation with increased adhesiveness as a result of a drastic change in their pattern of gene expression that includes the induction of E-cadherin,

occludin and several other adhesion proteins.[7] Both C-18 side chain analogues induced a similar morphological change as 1α,25(OH)$_2$D$_3$, promoting the formation of compact epithelioid cell islands, but again the analogue with the longer side chain (**2b**) was less efficient (Fig. 4A). Likewise, compound **2a** and 1α,25(OH)$_2$D$_3$ were equipotent in increasing the cellular content of E-cadherin, a hallmark of the differentiated phenotype, while the **2b** analogue was less potent (Fig. 4B). In agreement with this, analogue **2a** as well as 1α,25(OH)$_2$D$_3$, but not analogue **2b**, increased VDR expression (Fig. 4B).

Interestingly, introduction of a side chain at position C-18 led to an interesting decrease of calcemic activity. Indeed, when compared to 1α,25(OH)$_2$D$_3$, at least 600-fold higher doses of the 7- or 8-membered C-18 side chain analogues could be administered on a daily basis in NMRI vitamin D-replete mice (Table 1). This low calcemic activity makes these compounds, especially compound **2a**, appealing for therapeutic application.

Conclusions

We describe improved syntheses of two des-side chain analogues of 1α,25-dihydroxyvitamin D$_3$ with substituents at C-18. In the VDR structural study we demonstrated that the 7-membered side chain introduced at position C-18 in compound **2a** adopted the same orientation in the ligand binding pocket as the side chain of 1α,25-dihydroxyvitamin D$_3$ with maintenance of the hydrogen bonds that form the anchoring points of the ligand. Mutational analysis confirmed the interactions of compound **2a** with the amino acids lining the VDR-ligand binding pocket as determined in the crystallization study. Despite the fact that analogue **2a** fitted well in the VDR binding pocket, it displayed a

weak binding to VDR and homologation of the side chain further decreased the affinity. Nevertheless both des-side chain analogues of 1α,25-dihydroxyvitamin D_3 possessed significant antiproliferative and prodifferentiating properties with greatly reduced calcemic effects. This biological profile makes these analogues, and especially compound **2a**, potential candidates for the treatment of hyperproliferative disorders such as breast or colon cancer.

Experimental section

Chemistry.[8] In addition to NMR, HPLC analysis was used to determine the purity (>95%) of vitamin D analogues.

20(17→18)-abeo-3-(Triethylsilyl)-1α-[(triethylsilyl)oxy]-25-hydroxy-22-homo-21-norvitamin D_3 (2a-TES). A solution of *n*-BuLi (0.45 mL, 1.14 mmol, 2.5 M in hexanes) was added to a solution of phosphine oxide **3** (0.702 g, 1.204 mmol) in dry THF (8 mL) at -78 °C. The deep red solution was stirred for 1 h. A solution of ketone **4** (0.063 g, 0.277 mmol) in dry THF (8 mL) was added dropwise. The reaction mixture was stirred in the dark at -78 °C for 3 h and at -30 °C for 4 h. H_2O (0.5 mL) was added and the resulting mixture was concentrated to give a residue which was dissolved in Et_2O (100 mL). The combined organic phase was washed with saturated $NaHCO_3$ (20 mL), brine (3x20 mL), H_2O (60 mL), dried, filtered, and concentrated. The residue was purified by flash chromatography (SiO_2, 2x15 cm, 6-12% Et_2O-hexanes) to give the protected analogue **2a-TES** [0.125 g, 85%, *Rf* = 0.8 (30 % EtOAc-hexanes), colorless oil].

20(17→18)-abeo-1α,25-Dihydroxy-22,23-dihomo-21-norvitamin D_3 (2a). HF-pyridine complex (10 drops) was slowly added to a solution of **2a-TES** (0.125 g, 0.194 mmol) in dry CH_3CN (6 mL), dry CH_2CL_2 (4 mL) and dry Et_3N (3 mL). The reaction mixture was stirred in the dark at rt for 1 h. Saturated $NaHCO_3$ (30 mL) was added slowly and the aqueous layer was extracted with Et_2O (4x20 mL). The combined organic layer was washed with brine (2x25 mL), dried, filtered and concentrated. The residue was purified by flash chromatography (SiO_2, 1.5x15 cm, 10-12% *i*-PrOH-hexanes) to give **2a** [0.079 g, 98%, *Rf* = 0.4 (20% *i*-PrOH-hexanes), white solid].

20(17→18)-abeo-3-(Triethylsilyl)-1α-[(triethylsilyl)oxy]-25-hydroxy-22,23-dihomo-21-norvitamin D_3 (2b-TES). A solution of ***n***-BuLi (0.41 mL, 1.02 mmol, 2.5 M in hexanes) was added to a solution of phosphine oxide **3** (0.627 g, 1.076 mmol) in dry THF (5 mL) at -78 °C. The deep red solution was stirred for 1 h. A solution of ketone **7** (0.050 g, 0.17 mmol) in dry THF (5 mL) was added dropwise. The reaction mixture was stirred in the dark at -78 °C for 2 h and at -55 °C for 4 h. H_2O (0.5 mL) was added. Concentration gave a residue which was dissolved in Et_2O (100 mL). The combined organic phase was washed with saturated $NaHCO_3$ (20 mL), saturated NaCl (3x20 mL), H_2O (60 mL), dried, filtered, and concentrated. The residue was purified by flash chromatography (SiO_2, 2x15 cm, 6-12% Et_2O-hexanes) to give protected analogue **2b-TES** [0.091 g, 82%, *Rf* = 0.8 (30 % EtOAc-hexanes), colorless oil].

20(17→18)-abeo-1α,25-Dihydroxy-22,23-dihomo-21-norvitamin D_3 (2b). HF-pyridine complex (10 drops) was slowly added to a solution of **2b-TES**

(0.085 g, 0.136 mmol) in dry CH_3CN (3 mL), dry CH_2Cl_2 (1 mL) and dry Et_3N (1 mL). The reaction mixture was stirred in the dark at rt for 1.5 h. Saturated $NaHCO_3$ (30 mL) was added slowly and the aqueous layer was extracted with Et_2O (4x20 mL). The combined organic layer was washed with brine (2x25 mL), dried, filtered and concentrated. The residue was purified by flash chromatography (SiO_2, 1.5x15 cm, 10-12% *i*-PrOH-hexanes) to give **2b** [0.05 g, 95%, *Rf* = 0.5 (30% *i*-PrOH-hexanes), white solid].

Details on the syntheses of compounds **3**, **6a**, **6b**, **6c**, **6d**, **6e**, **6f**, **6g**, **6**, **7a** and **7** are described in the Supplementary Material.

Structural analysis of hDVR complexed to compound 2a, biological activity and electrospray ionization mass spectrometry are shown in the supplementary material.

Figure legends

Figure 1. Chemical structure of 1α,25$(OH)_2D_3$ and 20(17→18)-abeo-analogues.

Figure 2. Conformation of the VDR-bound **2a** analogue. (A) Compound **2a** is shown it its F_O-F_C electron density omit map contoured at 3.0 σ. The ligand is shown in stick representation with carbon and oxygen atoms in green and red, respectively. (B) A stereo view of the ligand conformations of 1α,25$(OH)_2D_3$ (red) and compound **2a** (blue) in their ligand binding pockets. (C) Superposition of the VDR·**2a** (gray) and VDR·1α,25$(OH)_2D_3$ (yellow) complexes. The view is restricted to the region of the protein (H3, H7, H11, and H12), which contains the side chain of the ligand. Only residues closer

than 4.0 Å are shown. Leu309 and Tyr401for the compound **2a** complex and Leu230, Leu404, Leu414, and Phe422 for the·1α,25(OH)$_2$D$_3$ complex are shown for comparisons. The ligands are shown in stick representation in blue for analogue **2a** and red for 1α,25(OH)$_2$D$_3$, respectively. The hydrogen bonds formed by the 25-OH groups are shown in blue (compound **2a**) and red (1α,25(OH)$_2$D$_3$) dashed lines.

Figure 3. Transactivating potency of different VDR point mutants in COS-1 cells. Cells were stimulated with 1α,25(OH)$_2$D$_3$ or the analogue **2a**, each applied at their EC50-concentrations (6 x 10^{-9} M for 1α,25(OH)$_2$D$_3$ and 3 x 10^{-9} M for analogue **2a**). Open bars represent results for 1α,25(OH)$_2$D$_3$ and black bars for compound **2a**. Bars represent means and S.D. of three independent experiments.

Figure 4. Analogues **2a** and **2b** induce an adhesive epithelial phenotype in SW480-ADH cells. (A) Differentiation of SW480-ADH cells demonstrated by phase-contrast micrographs of cells treated with 10^{-7} M of each compound or vehicle for 48 h. A representative experiment is shown. (B) Western blot analysis of the expression of the expression of E-cadherin, VDR and β-actin (loading control) at 8 h and 48 h of treatment with 10^{-7} M of each compound. Numbers show the quantification of the E-cadherin induction (ratio of levels in treated *versus* untreated cells) after normalization to β-actin. A representative experiment is shown.

Protein Data Bank Accession Number - The accession number for the coordinates of the complex reported in this article is PDB ID (3P8X)

Acknowledgment. This study was supported by the Spanish Ministry of Education and Science (Grants SAF2007-60341, SAF2007-67205), European Union (MRTN-CT-2005-019496, NucSys), Xunta de Galicia (Projets INCITE08PXIB-209130PR, ACEUIC-2006/XA050), Consolider, Nanobiomed, Fondo de Investigaciones Sanitarias, Fonds voor Wetenschappelijk Onderzoek (FWO) – Vlaanderen (G.553.06 and G.0587.09), CNRS, INSERM, Université de Strasbourg, ANR and the European Commission Structural Proteomics in Europe SPINE2-Complexes (LSHG-CT-2006-031220). CESGA (Santiago, Spain) is acknowledged for computing time granted to research group of AM. For the structural analysis we would like to thank the staff of the beamlines at ESRF for the experimental assistance during data collection. We thank IGBMC mass spectrometry common service for the mass spectrometry analysis. DN thanks the Argentinian CONICET for a postdoctoral fellowship. SE-C thanks the Spanish MEC for an FPU fellowship. GE is a postdoctoral researcher for FWO. We thank Dishman Netherlands B.V. (Weesp, the Netherlands) for the gift of vitamin D_2.

Supporting Information Available: Experimental procedures and crystallographic information files. This material is available free of charge via the Internet at http://pubs.acs.org.

Figure 1. Chemical structure of 1α,25$(OH)_2D_3$ and 20(17→18)-abeo-analogues.

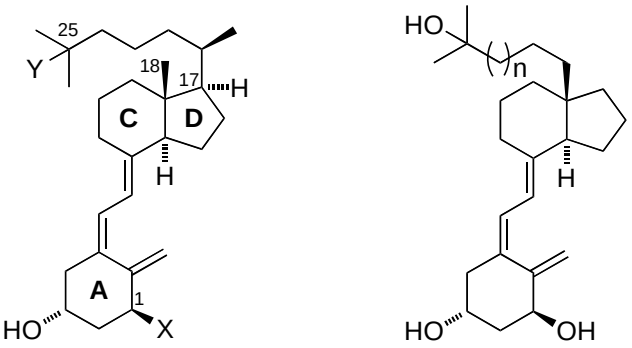

1a, X = Y = OH
1b, X = Y = H

2a, n = 4
2b, n = 5

Figure 2. Conformation of the VDR-bound **2a** analogue.

A

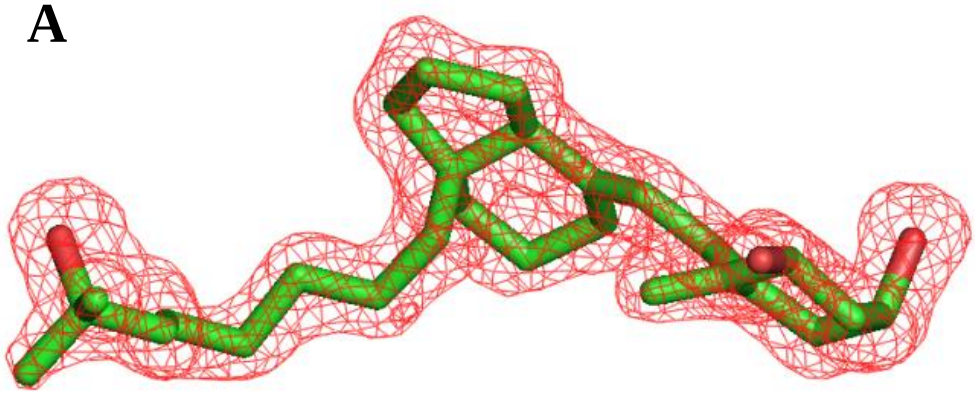

B

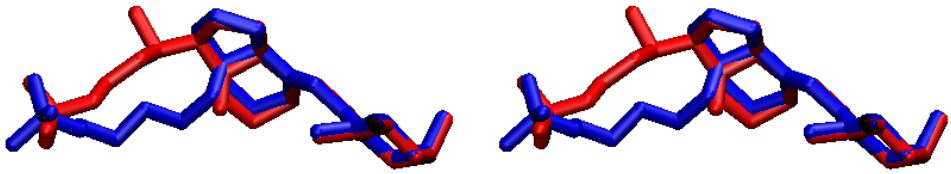

C

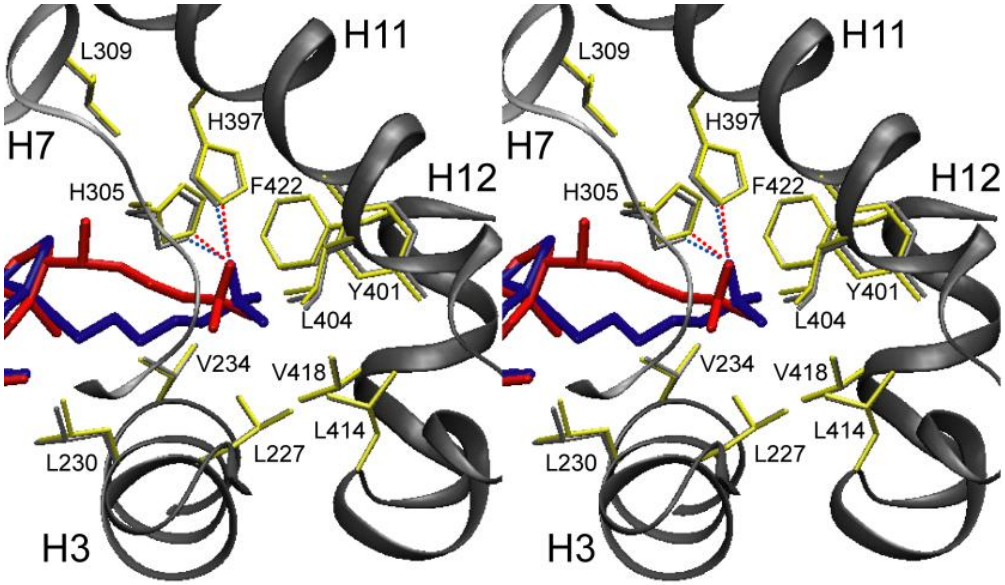
L309
H11
H7
H397
H305
F422
H12
Y401
L404
V234
V418
L414
L230
L227
H3
L309
H11
H7
H397
H305
F422
H12
Y401
L404
V234
V418
L414
L230
L227
H3

Figure 3. Transactivating potency of different VDR point mutants in COS-1 cells.

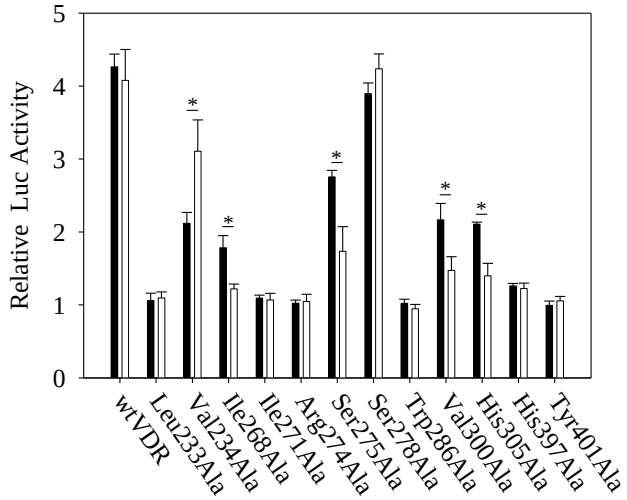

Figure 4. Analogues **2a** and **2b** induce an adhesive epithelial phenotype in SW480-ADH cells.

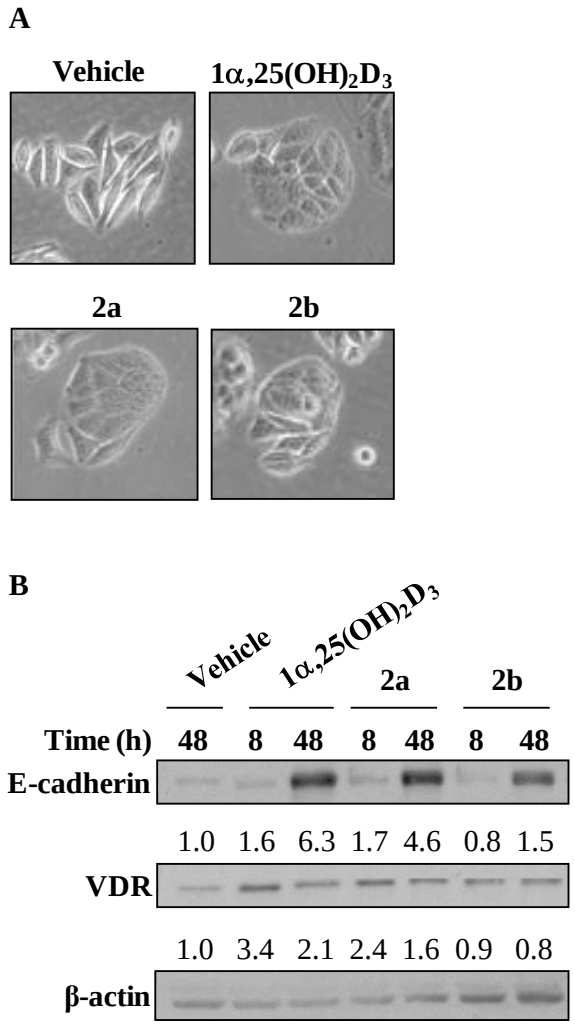

Scheme 1. Synthesis of **2a** and **2b**

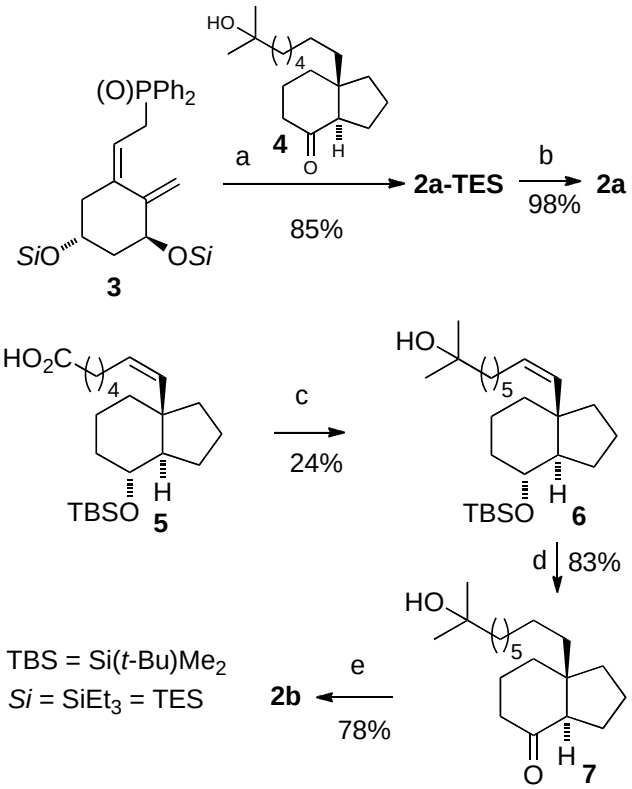

[a]Key: (a) *n*-BuLi, THF, -78 ºC; **4**. (b) HF-pyridine, CH_2Cl_2, (c) $LiAlH_4$, Et_2O, Δ; *p*-TsCl, DMAP, py, CH_2Cl_2, 0 ºC; NaCN, DMSO, 90 ºC; *i*-Bu_2AlH, CH_2Cl_2, 0 ºC; MeLi, Et_2O; PDC, CH_2Cl_2; MeLi, Et_2O. (d) 48% HF-Py, CH_3CN, CH_2Cl_2, Et_3N; H_2, 5% Pd-C, EtOAc; PDC, CH_2Cl_2. (e) **3**-Li-anion; HF-pyridine, CH_2Cl_2 (12 steps from **5**, 15.7% yield).

Table 1. *In vitro* binding affinities and antiproliferative activities and *in vivo*

calcemic effects of 1α,25(OH)$_2$D$_3$ and its 20(17→18)-abeo-1α,25-dihydroxy-21-norvitamin D$_3$ analogues.

	1α,25(OH)$_2$D$_3$	compound **2a**	compound **2b**
DBP K_D	5 x 10^8 M^{-1}	2 x 10^6 M^{-1}	4 x 10^{-6} M^{-1}
VDR K_D	2 x 10^{10} M^{-1}	2 x 10^9 M^{-1}	6 x 10^{-9} M^{-1}
Growth-inhibitory activity (EC50)	6 x 10^{-8} M	5 x 10^{-8} M	2 x 10^{-7} M
Calcemic activity (max applicable dose)	0.1 μg/kg/day	> 60 μg/kg/day	>100 μg/kg/day

The binding of 1α,25(OH)$_2$D$_3$ and the compounds **2a** and **2b** to human DBP and pig VDR was expressed by their dissociation constants. The antiproliferative effects of 1α,25(OH)$_2$D$_3$ and its analogues on MCF-7 cells were expressed as the concentrations required for the half-maximal inhibition of [^{3}H]thymidine incorporation. The calcemic activity of 1α,25(OH)$_2$D$_3$ and analogues **2a** and **2b** was determined in mice by intraperitoneal injections during 7 consecutive days. This activity was expressed as the maximal dose that could be administered without exceeding a serum calcium concentration observed when mice were treated with 0.1 μg/kg/day 1α,25(OH)$_2$D$_3$.

References

(1) Eelen, G.; Gysemans, C.; Verlinden, L.; Vanoirbeek, E.; De Clercq, P. J.; Van Haver, D.; Mathieu, C.; Bouillon, R.; Verstuyf, A. Mechanism and potential of the growth-inhibitory actions of vitamin D and analogs. *Curr. Med. Chem.* **2007**, *14*, 1893-1910.

(2) (a) Grue-Sorensen, G.; Hansen, C. M. New 1α,25-dihydroxy vitamin D_3 analogues with side chains attached to C-18: synthesis and biological activity. *Bioorg. Med. Chem.* **1998**, *6*, 2029-2039. (b) Cornella, I.; Perez, S. J.; Mouriño, A.; Sarandeses, L. A. Synthesis of new 18-substituted analogues of calcitriol using a photochemical remote functionalization. *J. Org. Chem.* **2002**, *67*, 4707-4714. (c) Nilsson, K.; Valles, M. J.; Castedo, L.; Mouriño, A. Synthesis and biological evaluation of 18-substituted analogs of 1α,25-dihydroxyvitamin D_3. *Bioorg. Med. Chem. Lett.* **1993**, *3*, 1855-1858.

(3) Moman, E.; Nicoletti, D.; Mouriño, A. Synthesis of novel analogues of 1α,25-dihydroxyvitamin D_3 with side chains at C-18. *J. Org. Chem.* **2004**, *69*, 4615-4625.

(4) Baggiolini, E. G.; Iacobelli, J. A.; Hennessy, B. M.; Batcho, A. D.; Sereno, J. F.; Uskokovic, M. R. Stereocontrolled total synthesis of 1α,25-dihydroxycholecalciferol and 1α,25-dihydroxyergocalciferol. *J. Org. Chem.* **1986**, *51*, 3098-3108 and references therein.

(5) Rochel, N.; Moras, D. Ligand binding domain of vitamin D receptors. *Curr. Top. Med. Chem.* **2006**, *6*, 1229-1241.

(6) For details, see supplementary material.

(7) Palmer, H. G.; Gonzalez-Sancho, J. M.; Espada, J.; Berciano, M. T.; Puig, I.; Baulida, J.; Quintanilla, M.; Cano, A.; de Herreros, A. G.; Lafarga, M.; Munoz, A. Vitamin D_3 promotes the differentiation of colon carcinoma cells by the induction of E-cadherin and the inhibition of beta-catenin signaling. *J. Cell Biol.* **2001**, *154*, 369-387.

TABLE OF CONTENTS GRAPHIC (Word Style “SN_Synopsis_TOC”).

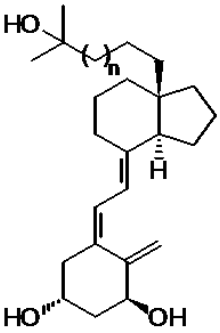
HO
n
H
HO
OH

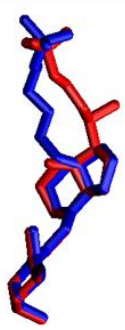

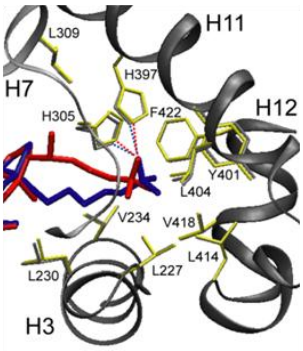
L309
H11
H397
H7
H305
F422
H12
Y401
L404
V234
V418
L414
L230
L227
H3